Fatigue Crack Length Estimation and Prediction using Trans-fitting with Support Vector Regression

Myeongbaek Youn[1], Yunhan Kim[2], Dongki Lee[3], Minki Cho[4], and Byeng D. Youn[5*]

[1,2,5]*Department of Mechanical and Aerospace Engineering, Seoul National University, Seoul, 08826, Republic of Korea*
mbyun1420@snu.ac.kr
gav0304@snu.ac.kr
bdyoun@snu.ac.kr

[3,4]*Material & Production Engineering Research Institute, LG Electronics Inc., Gyeonggi-do 17709, Republic of Korea*
dongki2.lee@lge.com
minki.cho@lge.com

[5]*Institute of Advanced Machines and Design, Seoul National University, Seoul 08826, Republic of Korea*
bdyoun@snu.ac.kr

[5] *OnePredict Inc, Seoul, 08826, Republic of Korea*
bdyoun@snu.ac.kr

ABSTRACT

A method is described in this paper for crack propagation prediction using only the initial crack length of the target specimen. The proposed method consists of two parts: (1) crack length estimation using support vector regression (SVR) and (2) crack length prediction using a new trans-fitting method. Features based on the filtered wave signals were defined and a model was constructed using the SVR method to estimate the crack length. The hyper-parameters of the SVR model were selected based on a grid search algorithm. Prediction of the crack length was based on the previous crack length, which was estimated based on the wave signals. In this step, a newly proposed trans-fitting method was applied. The proposed trans-fitting method updated the selected candidate function to translocate the trend of crack propagation based on the training dataset. By translocating the trends to the estimated crack length of the target specimen, the crack propagation could be predicted. The proposed method was validated by comparison with given specimens. The results show that the proposed method can estimate and predict the crack length accurately.

*Corresponding author: Byeng D. Youn (e-mail: bdyoun@snu.ac.kr)

1. INTRODUCTION

Recently, safety and reliability of structures has received significant research attention, with the goal of preventing catastrophe and unexpected failure. To achieve this goal, maintenance strategies have changed from conventional corrective or preventive maintenance to condition-based maintenance (CBM) (Lee, 2014). CBM is a maintenance strategy that continuously monitors the condition of a target system through real-time monitoring. In addition, real-time monitoring for structural defects is called structural health monitoring (SHM) (Tinga & Loendersloot, 2014). Because its benefits include real-time damage detection and forecasting of remaining service life, much research has examined SHM's applications in various fields, such as civil engineering (Brownjohn, 2006), aerospace, and mechanical engineering (Adams, White, Rumsey, & Farrar, 2011; Staszewski, Mahzan, & Traynor, 2009).

Ultrasonic guided wave signals have been used as damage assessment tools for SHM, primarily due to their low energy loss in long-distance propagation (Janapati, Kopaftopoulos, Li, Lee & Chang, 2016; Qiu, Liu, Qing, & Yuan, 2013). Ultrasonic guided wave signals make damage assessment effective because they can quantify the change of the signal caused by a crack, delamination, or corrosion. In particular, the lamb wave signal, an ultrasonic guided wave signal in the form of elastic perturbation, showed good performance in structural integrity evaluation and fatigue life prediction of a thin plate or shell structure (Liu, Frangopol, & Kwon, 2010;

Kessler, Spearing, & Soutis, 2002). A considerable amount of literature related to prognosis studies of cracks for cyclic loads based on lamb wave has been published. Coelho (2007) used a one class SVM classifier with a lamb wave signal to identify fatigue damage specimens exposed to cyclic loading. Peng et al. (2015) constructed a real-time composite fatigue life prognosis framework using a Bayesian-inference-based updating model based on the mechanical stiffness of the specimen. Neerukatti et al. (2016) performed a prognosis for crack growth using particle filters (PF) with lamb wave-based damage localization. However, most previous research has the disadvantage of requiring a significant amount of information about the target specimen to make an accurate crack propagation model, which is a critical problem in terms of both time and cost when applied in industrial sites. In this paper, therefore, a method is proposed to make a crack propagation model that is accurate, but that uses only a small amount of information from the target specimen. Verification for the proposed method used the dataset from the 2019 PHM Conference Data Challenge.

In the 2019 PHM Conference Data Challenge, fatigue crack lengths were estimated and predicted for aluminum lap joint specimens under dynamic tensile loading conditions. The goal of the challenge was to (1) estimate crack lengths for target cycles of different specimens using a quantification model, and (2) predict crack length for subsequent target cycles based on estimation results. Training and validation datasets were given, along with the wave signals and crack lengths for each cycle. With limited information about the experiment (e.g., details of material and structural geometry), the data-driven approach was considered first, since the change in the wave signal contains the most essential information about the crack length. Therefore, in the proposed method, support vector regression (SVR) was used first to construct a quantitative model of the crack length and the change in the wave signal for the training dataset. Then, a regression model was used to estimate the crack length for the validation specimens. Finally, crack length prediction for the validation data in the absence of wave signals was performed using the proposed trans-fitting method.

The rest of the paper is organized as follows. Section 2 introduces the problem and the scoring process. Section 3 describes the process proposed to estimate and predict crack length. Section 4 shows the validation results of the proposed method. Conclusions and suggestions for future work are presented in Section 5.

2. PROBLEM DESCRIPTION

This section briefly introduces the problem outlined for the 2019 PHM Conference Data Challenge. Information about the problem includes: (1) problem definition, (2) a description of the given dataset, and (3) the scoring process.

2.1. Problem definition

For this data challenge, the crack length of an aluminum specimen was to be estimated and predicted using signals from piezoelectric (PZT) sensors. The system under investigation in this competition is shown Figure 1. PZT sensors are mounted at both the actuator and receiver to measure the wave signals. The distance between the actuator and the receiver is 161mm. When a crack initiates across the wave propagation path, the received signal is changed. This phenomenon can be analyzed to estimate the crack length. Based on the relationship between the fatigue crack and the wave signal, the main objectives of this challenges were to (1) estimate the crack length of the validation set in a given cycle, and (2) predict the crack length in a given cycle without signal information.

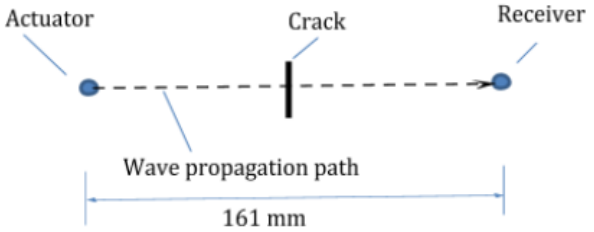

Figure 1. Schematic illustration of the crack-sensing mechanism

2.2. Description of the datasets

For the competition, datasets of eight specimens (named T1 through T8) were given; divided into two groups. The first was a training dataset, consisting of data from six specimens (T1-T6). The second was the validation dataset consisting of data from two specimens (T7-T8). Each specimen was subjected to tensile dynamic loading, which was performed with a hydraulic material testing machine working at 5 Hz under room temperature. While constant amplitude loading was applied in the training datasets and one of the specimens in the validation dataset (T7), variable loading was applied to the other specimen in the validation dataset (T8). Each dataset consisted of cycles and crack lengths measured by an optical microscope. Additionally, training datasets included wave signals acquired from all provided cycles; however, validation datasets provided wave signals only for the initial cycles.

Table 1. Summary of training dataset

Specimen	Number of cycle data	Number of wave signal dataset	Loading condition
T1	7	7	Constant amplitude
T2	3	3	Constant amplitude
T3	10	10	Constant amplitude
T4	8	8	Constant amplitude
T5	4	4	Constant amplitude
T6	6	6	Constant amplitude

Table 2. Summary of validation dataset

Specimen	Number of cycle data	Number of wave signal dataset	Loading condition
T7	8	4	Constant amplitude
T8	10	5	Variable amplitude

2.3. Scoring process

Three penalty functions were applied to score the proposed estimation and prediction of the crack length; (1) a time penalty function, (2) an asymmetric penalty function, and (3) a monotonicity penalty function. The constant parameters of the penalty functions suggested here used the same values as the values used in the 2019 PHM Conference Data Challenge. The first penalty function was set up to place more weight on the error at a later crack length than on the error at the initial crack length; this penalty was defined as

$$T(i) = 2 + 10x_i \tag{1}$$

where x_i is the true crack length. This penalty means that it is more important to predict the crack as it gets closer to the failure time of the structure. Underestimation and overestimation of the crack length were penalized differently by the second penalty function. This is because underestimation of the crack length is riskier than overestimation of the crack length in the real applications. The asymmetric penalty function was defined as

$$A(i) = \begin{cases} \exp\left\{\dfrac{|\tilde{x}_i - x_i|}{0.5}\right\} - 1; & (\tilde{x}_i - x_i) \geq 0 \\ \exp\left\{\dfrac{|\tilde{x}_i - x_i|}{0.2}\right\} - 1; & (\tilde{x}_i - x_i) < 0 \end{cases} \tag{2}$$

where x_i is the true crack length and $\tilde{x}_i$ is the estimated or predicted crack length. The third penalty function was devised to penalize the trend of breaking monotonicity along the cycle, which cannot occur physically. The monotonicity penalty function was defined as follows

$$M(i) = \begin{cases} 1 + 10(|\tilde{x}_i - \tilde{x}_{i-1}|); & (\tilde{x}_i - \tilde{x}_{i-1}) < 0 \\ 1; & (\tilde{x}_i - \tilde{x}_{i-1}) \geq 0 \end{cases} \tag{3}$$

where $\tilde{x}_i$ is the ith estimated or predicted crack length and $\tilde{x}_{i-1}$ is the $i-1$th estimated or predicted crack length. The overall penalty score was calculated by multiplying the three penalty functions.

$$S(i) = T(i) \times A(i) \times M(i) \tag{4}$$

Using the overall penalty score, the performance of the proposed method was evaluated for its ability to accurately estimate and predict crack lengths. A lower score means that the result of the proposed method is more accurate.

3. PROPOSED METHOD

Our proposed method for crack length estimation and prediction is described in this section. The method for crack length estimation is explained in the first subsection; the method for predicting the crack length using the proposed trans-fitting method is shown in the second subsection.

3.1. Crack length estimation based on wave signals

The proposed method for crack length estimation is based on a regression model. To construct the regression model, the features from the wave signals were first defined (Ahmad, Khan, Islam, & Kim, 2019). Since wave signals are measured with noise, the noise signals were filtered to effectively extract the features. Then, the regression model was built to estimate the crack length via the support vector regression (SVR) method. A detailed description of the proposed method follows.

3.1.1. Preprocessing

The wave signals for the fatigue test were measured under a noisy environment. When signals are measured in a noisy environment, de-noising is necessary to effectively extract crack-related features. Further, the frequency components of the received signals mainly exist in a certain band in the frequency domain, since the center frequency of the actuator signals is 200 kHz. Therefore, a band-pass filter was applied to filter the noise and extract the useful signals from the raw signals (Bozchalooi & Liang, 2008). Figure 2 shows the frequency components of the received signals from the T2 specimen under 50000 cycles and 72000 cycles. As shown in Figure 2, the frequency components of the received signals are located in the frequency band between 100 kHz and 500 kHz. Therefore, a fifth-order Butterworth band-pass filter (Oppenheim, 1999) was designed with a bandwidth of 100-500 kHz. Figure 3 shows the raw signals and the filtered signals from the receivers of specimen T2 under 50000 cycles and 72000 cycles. The designed band-pass filter can filter the noisy signals to extract useful signals, as can be seen in the figure.

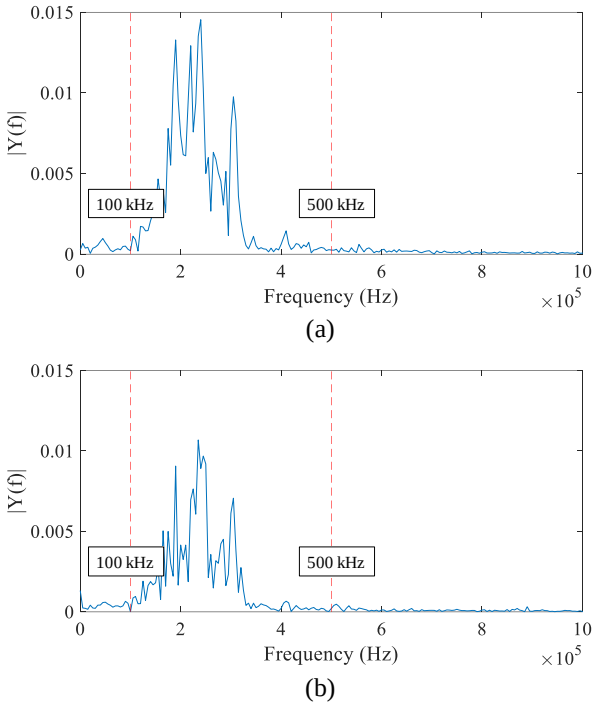

Figure 2. Received signals from specimen T2 in the frequency domain: (a) 50000 cycles, (b) 72000 cycles

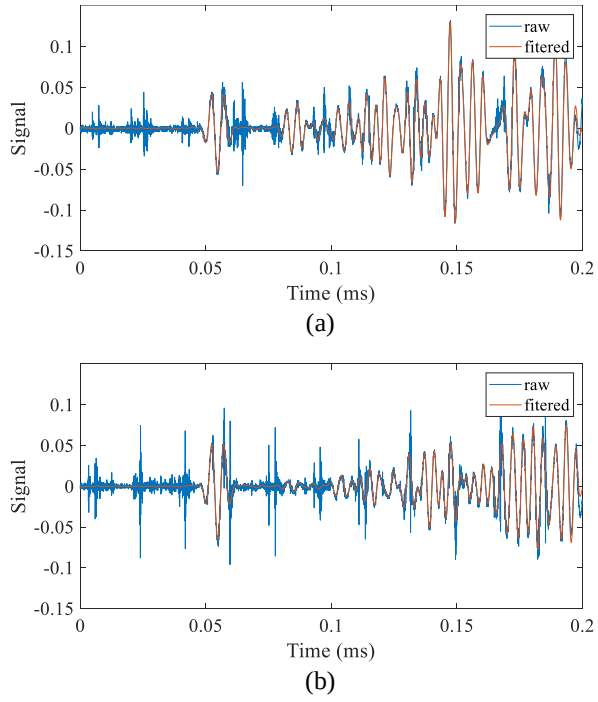

Figure 3. Raw signals and filtered signals from specimen T2: (a) 50000 cycles, (b) 72000 cycles

3.1.2. Feature extraction

Next, the meaningful features for crack length estimation using the filtered signals were defined. Since the actuator signal passes through the crack of the specimen, the crack distorts the received signal (Yang, Ng, & Kotousov, 2018). Also, a severe crack has a greater effect on the distortion of the received signal. Therefore, the distortion of the received signal was quantified as a feature extraction step for the proposed crack length estimation. A sinusoidal wave with the first four cycles of the filtered signal was used because the actuator signal consists of the four cycles with a center frequency of 200 kHz (i.e., 400 samples with a sampling frequency of 20 MHz). Then, four features were defined from the filtered signal, specifically: (1) root mean square (RMS), (2) standard deviation, (3) metric of orthogonality, and (4) magnitude of the component at 300 kHz. A detailed description of the features follows.

(1) Root mean square (RMS)

The first feature is the root mean square (RMS) of the filtered signal. This feature is based on the phenomena of the reduction in the power of the filtered signal that arises due to the existence of the crack in the specimen. Therefore, the first feature decreases as the crack length increases. The first feature is expressed as

$$Feature1 = \frac{1}{N}\sum_{n=1}^{N}(x[n])^2 \tag{5}$$

where n is discrete time, N is the number of samples for the signal, and $x[n]$ is the filtered signal.

(2) Standard deviation

The second feature is the standard deviation of the filtered signal. The standard deviation of the signal physically indicates the power dispersion of the signal. This feature is based on the same relationship between the filtered signal and the existence of the crack. The second feature is also expected to decrease as the crack length increases. The second feature is defined as

$$Feature2 = \sqrt{\frac{1}{N}\sum_{n=1}^{N}\left(x[n] - \overline{x[n]}\right)^2} \tag{6}$$

where $\overline{x[n]}$ is mean of the signal $x[n]$.

(3) Metric of orthogonality

The third feature is the metric of the orthogonality of the signal. This feature quantifies the difference of the signals observed between undamaged and damaged specimens. As the crack size increases, the signal becomes increasingly different from the signal of the undamaged specimen; this is because a severe crack results in a large distortion of the signal. The metric of the orthogonality is formulated as

$$Feature3 = \frac{\sum_{n=1}^{N}(x[n]x_0[n])}{\sum_{n=1}^{N}(x[n])^2 \sum_{n=1}^{N}(x_0[n])^2} \quad (7)$$

where $x_0[n]$ is the signal from the undamaged specimen.

(4) Magnitude of the component at 300 kHz

The features defined in the prior subsections are in the time domain. The change of signal that is due to the crack in the frequency domain can also be quantified. The frequency component at 300 kHz monotonically increases as the size of the crack grows. The frequency component at 300 kHz physically means a sideband component arises due to the crack. Therefore, the fourth feature was defined as the magnitude of the sideband components at 300 kHz. The fourth feature is expressed as

$$Feature4 = X[k_{300}] \quad (8)$$

where X is the magnitude of the signals from Fourier transform in the frequency domain and k_{300} is the discrete frequency of 300 kHz.

To summarize, four features were defined for crack length estimation. However, while each specimen had about the same actuating signal, there was variation in the received signals. To reduce such variations, the value of each feature was normalized using the feature from an undamaged specimen. A summary of the features chosen for crack length estimation is given in Table 3.

Table 3. Summary of the features used for the crack estimation

Features	Physical meaning
Root mean square	Power of the signals
Standard deviation	Power dispersion of the signals
Metric of orthogonality	Difference from the undamaged signals
Magnitude of component at 300 kHz	Power in the frequency domain

3.1.3. Regression

Finally, a regression model was constructed using the defined features to estimate the crack length. SVR is a regression method that uses the same principle as the support vector machine (SVM) method. For the training dataset consisting of feature vectors from the signals and the measured crack lengths, the SVR method formulates the regression model as

$$\hat{a} = \omega^T \phi(z) + \omega_0 \quad (9)$$

where $\hat{a}$ is an estimated crack length, z is a feature vector, $\phi(\cdot)$ is a non-linear mapping function, ω is a weight vector, and ω_0 is a bias term. To find the optimal weight vector and bias term, the objective function should be minimized as follows:

$$\text{minimize } C\sum_{n=1}^{N}(\xi_n^u + \xi_n^l) + \frac{1}{2}\|\omega\|^2 \quad (10)$$

$$\text{subject to } \begin{cases} a_n \le \omega^T\phi(z) + \omega_0 + \epsilon + \xi_n^u \\ a_n \ge \omega^T\phi(z) + \omega_0 - \epsilon - \xi_n^l \\ \xi_n^u, \xi_n^l \ge 0 \end{cases} \quad (11)$$

where N is the number of samples in the training dataset, C is a penalty parameter, ϵ is a tolerance parameter, ξ_n^u and ξ_n^l are slack variables. This formulation can be converted to a dual problem using a kernel function (Bishop, 2006)

The performance of the SVR method depends on the hyper-parameters, such as the type of the kernel, kernel parameter, regularization parameter, and so on (Benkedjouh, Medjaher, Zerhouni, & Rechak, 2013). To select the best hyper-parameters, grid-search algorithms were exploited (Salcedo-Sanz, Ortiz-Garcı, Pérez-Bellido, Portilla-Figueras, & Prieto, 2011). Figure 4 shows the comparison between the true crack lengths of the training specimens (specimens T2, T3, and T4) and the crack lengths estimated from the SVR model. In terms of the hyper-parameters, the radial basis function (RBF) kernel of the kernel parameter was selected as 1.0, and the regularization parameter was selected as 100.0 through use of the grid-search method. As shown in Figure 4, it was found that the proposed SVR model could properly estimate the crack lengths. The root mean square error from the regression model is 1.65.

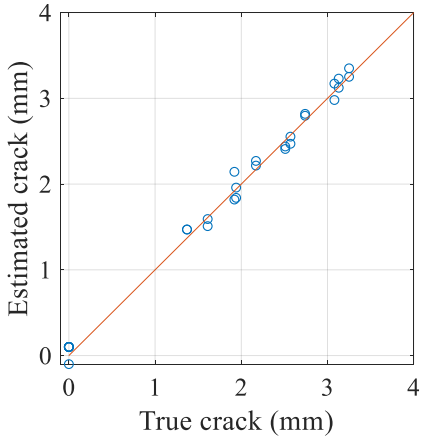

Figure 4. True and estimated crack lengths for the training specimens

3.2. Crack length prediction using the proposed trans-fitting method

The proposed method for crack length prediction is based on a novel trans-fitting method. The basic idea of trans-fitting is to extract the crack propagation trend from the training

dataset and adapt the trend to predict the crack lengths of the validation set. In the absence of a wave signal, the task of predicting the crack length for a target cycle is an extrapolation process. Traditionally, crack length prediction has been done using physics-based models, such as Paris' law (Paris & Erdogan, 1963), the Forman equation (Forman, Kearney, & Engle, 1967), or the Walker equation (Walker, 1970). However, it is difficult to predict crack length using those physics-based models without given information, such as the shape of the initial crack, specimen geometry, and material properties. This is because the physics-based models using insufficient information can result in an inaccurate crack length. For this reason, a new method is proposed in this work, called trans-fitting. The trans-fitting method is carried out in four steps, as illustrated in Figure 5. A detailed description of the proposed method follows.

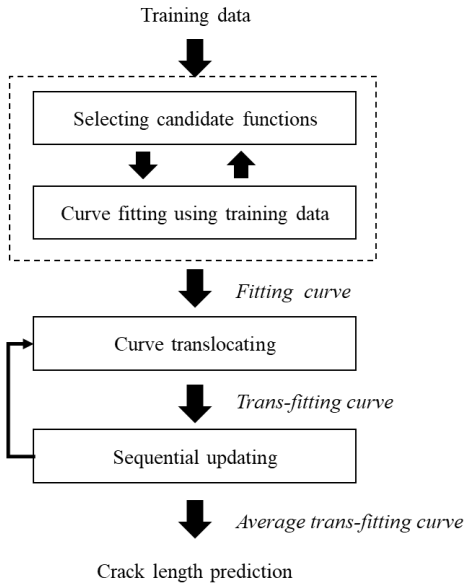

Figure 5. Flowchart of the proposed trans-fitting method

3.2.1 Selecting candidate functions

The first step in the proposed method is to select candidate functions to fit the crack propagation trends observed in the training datasets. Among the various candidate functions, functions were selected based on two statistical indicators for evaluation of their goodness-of-fit. The first indicator is the sum of square error (SSE). The SSE is defined as

$$SSE = \sum_{i=1}^{L} (\hat{a}(N^i, \theta) - a^i)^2 \qquad (12)$$

where θ represents the parameters of the candidate function, L is the number of samples, N^i is the ith number of cycles, a^i is the ith measured crack length, and $\hat{a}$ is the crack length calculated from the fitting curve of the selected candidate function. This indicator quantifies the difference between the trend determined from the training dataset and from the fitting curve to the selected candidate function. The second indicator is the degree of freedom for error (DFE). The DFE can be expressed as

$$DFE = L - P \qquad (13)$$

where L is the number of samples and P is the number of parameters in the candidate function. This indicator is used to check the risk of overfitting. For example, a small DFE value means that there is a risk of overfitting with the results of the candidate function (Walker, 1940). Thus, with a small DFE, it cannot be guaranteed that the fitting curve of the selected candidate function translocates the crack propagation trend properly. Table 4 shows the results of these two statistical indicators for the candidate functions of the training dataset for specimens T3 and T4. For the candidate functions, various kinds of candidate functions were considered, such as first-order polynomial (Poly1), second-order polynomial (Poly2), exponential function (Exp1), sum of two exponential functions (Exp2), Gaussian function (Gaussian1), sum of two Gaussian functions, power function (Power1), power function with bias term (Power2), and sum of exponential and Gaussian function (Exp1+Gaussian1).

Table 4. Goodness-of-fit results for specimens T3 and T4

	T3		T4	
Candidates	SSE	DFE	SSE	DFE
Poly1	0.1311	5	5.0581	5
Poly2	0.1183	4	1.0960	4
Exp1	0.2298	5	1.2827	5
Exp2	***0.0639***	***3***	***1.0510***	***3***
Gaussian1	0.1497	4	155.42	4
Gaussian2	*0.0033*	*1*	*0.1976*	*1*
Power1	0.2011	5	1.5735	5
Power2	0.1223	4	1.8047	4
Exp1+Gaussian1	***0.1106***	***2***	***0.9878***	***2***

The results of the SSE show that the sum of two Gaussian models (Gaussian2) has the lowest value for both training datasets. However, the Gaussian 2 model was excluded from the candidate functions since the DFE for the Gaussian 2 model is 1; this means that the fitting curve is highly over-fitted and can thus fail to translocate crack propagation trends to the validation set. As a result, the sum of two exponential functions (Exp2) and the sum of the Gaussian model and exponential function (Exp1+Gaussian1) were selected; these are formulated as

$$\hat{a}(N^i, \theta) = \theta_1 \exp\left(-\left(N^i - \theta_2\right)^2\right) + \theta_3 \exp\left(\theta_4 N^i\right) + \theta_5 \qquad (14)$$

$$\hat{a}(N^i, \alpha) = \alpha_1 \exp\left(\alpha_2 N^i\right) + \alpha_3 \exp\left(\alpha_4 N^i\right) \qquad (15)$$

where θ_i is the parameter of the sum of the Gaussian model and exponential function, α_i is the parameter of the sum of two exponential functions, N^i is the number of cycles, and $\hat{a}$ is an estimated crack length.

3.2.2 Curve fitting using training data

The second step is fitting the training dataset to the candidate functions; this is performed concurrently with the previous step. This process was used to estimate the parameters of the candidate functions using nonlinear least-square optimization. The objective function consists of the error between the crack length calculated from the fitting curve to the selected candidate function and from the training dataset, with a regularized term for preventing overfitting, as shown in Eq. (16)

$$minimize \sum_{i=1}^{l} (\hat{a}(N^i, \theta) - a^i)^2 + \lambda \sum_{k=1}^{n} \theta_k^2 \qquad (16)$$

where θ and θ_k are parameters of the selected candidate function, N is the number of cycles, a is a measured crack length, and λ is a regularized parameter. Also, the trust-region algorithm (Conn, Gould, & Toint, 2000) is used for the nonlinear, least-square optimization algorithm.

3.2.3 Curve translocating

This step is translocating the crack propagation trend to match the estimated crack length determined from the SVR model. Translocating is performed by updating the parameters of the fitting curves based on the initial crack length of the target specimen. First, the parameters of the fitting curve – meaning the training crack propagation – were trend set as prior distributions. Second, the error model calculated using the initial crack length of the target and the value calculated by the fitting curve became the likelihood. Finally, the maximum a posterior (MAP) process was performed by maximizing the probability of the posterior distribution. As a result, the calculated posterior parameters determine the trans-fitting curve, which gives the crack propagation trend of the target specimen. The formulation of the MAP process is equivalent to minimizing Eq. (17), as

$$E_{\mathrm{MAP}}(\theta) = \frac{1}{2\sigma^2} \sum_{i=1}^{l} \{a_{\mathrm{SVR}_i} - a_{\mathrm{fit}}(N_i; \theta)\}^2 + \frac{\alpha}{2} \sum_{k=1}^{n} \theta_k^2 \qquad (17)$$

where θ and θ_k are the parameter of the fitting curve, N_i is the number of cycles, a_{fit} is the crack estimation derived from the fitting curve, a_{SVR} is the crack estimation from the SVR model, α is the prior standard deviation, and σ is the likelihood standard deviation. When the regularized parameter, λ, is equal to $\sigma^2\alpha$, the MAP process is equivalent to the nonlinear least square with a regularized term (Tipping, 2003). The translocated fitting curve is now called a trans-fitting curve.

As multiple training datasets were available, trans-fitting curves could be obtained for each training dataset. To get a more representative trend of the crack propagation, all of the trans-fitting curves were averaged. By taking the average, the variance from each training dataset is reduced, and the crack propagation trend becomes more representative. For example, in the case of using two training datasets (e.g., specimens T3 and T4), as shown in Figure 6, a fitted curve representing each crack propagation trend can be drawn, as shown by the blue solid line. These curves were translocated into the initial crack length position through the curve translocating process. Finally, using the average of the two trans-fitting curves, the average trans-fitting curve was calculated; this is shown as a solid red line.

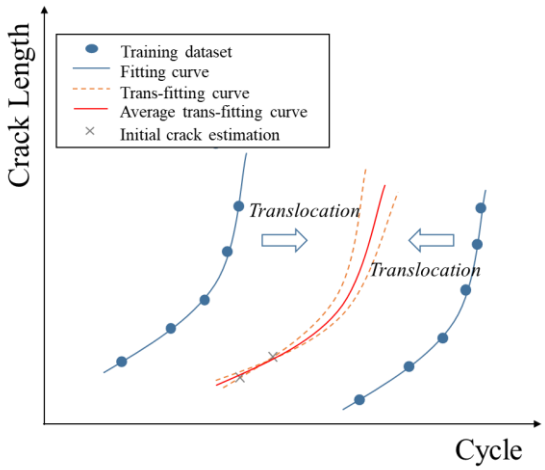

Figure 6. Curve translocating and trans-fitting curves

3.2.4 Sequential updating

Using the process outlined in the previous step, the newly predicted crack length was obtained for the target cycle. The newly predicted value from the average trans-fitting curve contains better predictive information than the results that were determined from a single trans-fitting curve. Therefore, to improve the results of the crack length prediction, the curve translocating process was repeated using the newly predicted crack length. Figure 7 shows the concept of sequential updating. For example, using the newly predicted crack length (as shown by the red-cross point in the figure), the curve translocating process was recalculated from the previous step containing the additional point. Through this process, a newly updated trans-fitting curve was obtained, as depicted by the orange line in the figure.

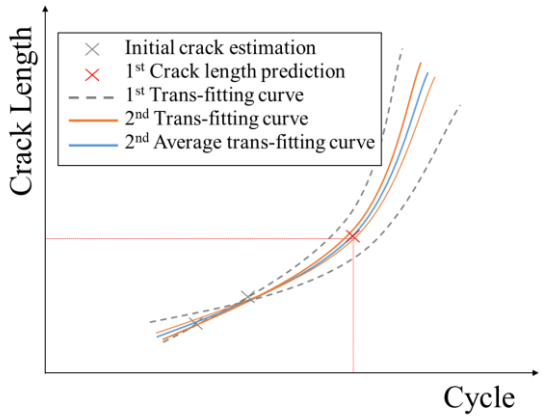

Figure 7. Sequential updating

4. RESULTS

This section describes how the proposed method was demonstrated using the two validation datasets. Within the hypothesis of the proposed method, crack propagation was predicted using only the initial crack length of a target specimen. The first validation dataset was performed in the same load condition to estimate the initial crack length of the target based on the wave signal and then to predict the crack propagation trend without the lamb wave signal. The second validation dataset was conducted to check the robustness of the load condition. Under the condition in which the training dataset was the same as in the first validation and the target specimen was exposed to variable loading, the initial crack length was estimated and then the crack propagation trend was predicted.

4.1. Validation 1: Specimen T7 under constant loading

The first step was to estimate the crack lengths based on the wave signals. A regression model was constructed using the SVR method. The proposed method for the crack estimation required signals from an undamaged specimen. By comparing the filtered wave signals under 36001, 40167 and 44054 cycles, it was decided that the crack was initiated between cycles 40167 and 44054. For that reason, the signal under the 40167 cycle was chosen as the undamaged specimen signal. With this information, the crack length could be estimated using the proposed method. The result of the estimated crack length is shown in Table 5.

Table 5. Estimated crack lengths for specimen T7

Cycles	36001	40167	44054	47022
Estimated crack (mm)	0	0	1.92	3.08
Ground truth (mm)	0	0	2.07	3.14
Penalty Score $S(i)$	0	0	25.36	11.69

Based on the crack length value estimated by the SVR method, the prediction process was then performed using the proposed trans-fitting method. The crack propagation trend was extracted from the training dataset (for specimens T3 and T4); these specimens have more data points than the target prediction points. First, based on the statistical indicators, the sum of two exponential functions model (Exp2) was selected for specimen T3 and the sum of Gaussian model and exponential function (Exp1+Gaussian1) was selected for specimen T4. The results of the goodness-of-fit for the two candidate functions are given in Table 6. Second, along with the results of the goodness-of-fit test, training datasets were fitted to each of the selected candidate functions.

Table 6. Goodness-of-fit results for specimen T7

	T3		T4	
Candidates	SSE	DFE	SSE	DFE
Exp2 (E2)	0.0639	3	1.051	3
Exp1+Gaussian1 (GE)	0.1106	2	0.9878	2

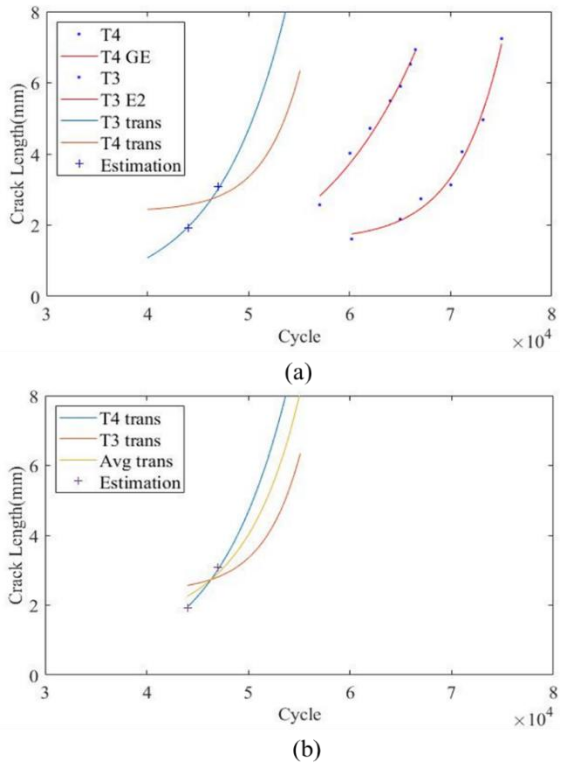

Figure 8. Results of the curve translocating process for specimen T7: (a) trans-fitting curves, (b) average trans-fitting curve

Third, the parameters of the fitting curve were updated. Figure 8 shows the results of the trans-fitting curves. As shown in Figure 8(a), E2 was fitted to the training dataset

from specimen T3 and GE was fitted to the training dataset from specimen T4. Then, the average trans-fitting curve was calculated using the average of the two trans-fitting curves, as shown in Figure 8(b). Finally, sequential updating was performed based on the crack length for the target cycle. Based on the first average trans-fitting curve, the results of sequential updating for the predicted crack length are shown in Figure 9.

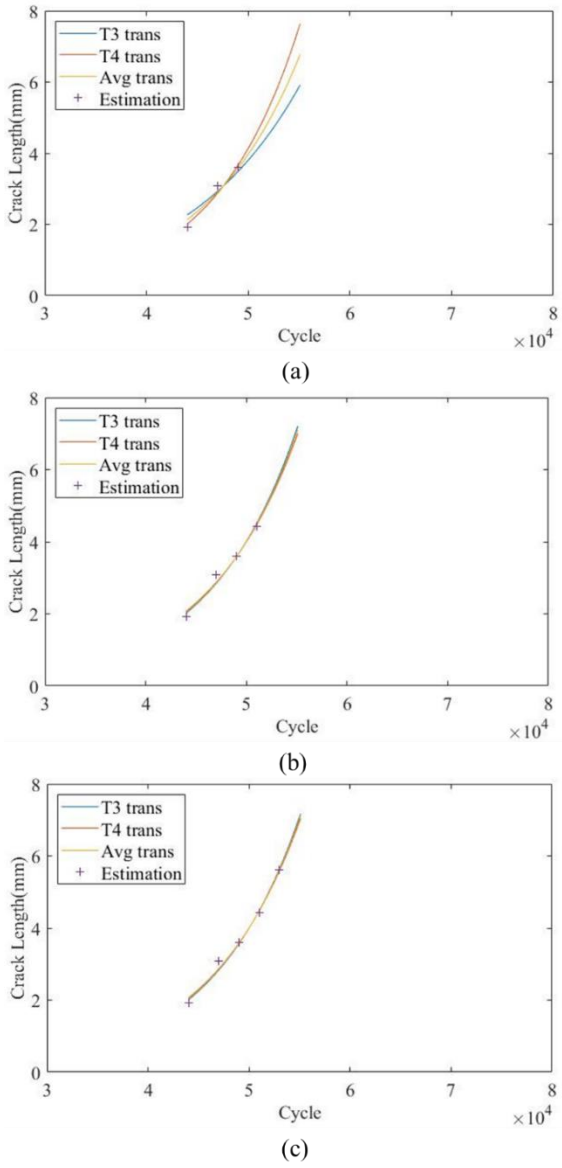

Figure 9. Sequentially updated curves for specimen T7: (a) average trans-fitting curve for the second iteration, (b) average trans-fitting for third iteration, (c) average trans-fitting for the fourth iteration

From Figure 8(b) to Figure 9(c), there are four average trans-fitting curves. Each average trans-fitting curve can predict the crack lengths for the target cycles after the cycle used in the sequential updating process, as shown in Table 7. Based on the assumption that using all of the predicted crack lengths results in a smaller uncertainty than the predicted value from a single average trans-fitting curve, the average value for all of the predicted crack lengths was adopted as the last prediction value.

Table 7. Predicted crack lengths for specimen T7

Cycle	49026	51030	53019	55031
1st average trans-fitting curve	3.59	4.55	5.95	8.03
2nd average trans-fitting curve		4.42	5.44	6.73
3rd average trans-fitting curve			5.62	7.05
4th average trans-fitting curve				7.05
Final average value	3.59	4.48	5.67	7.21
Ground truth (mm)	3.56	4.48	5.05	7.22
Penalty Score $S(i)$	2.33	43.90	128.92	3.80

4.2. Validation 2: Specimen T8 under variable loading

As in the validation for specimen T7, first, the crack lengths were estimated based on the wave signals. The proposed method for crack length estimation needs to select the wave signals from an undamaged specimen. By comparing the filtered wave signals under 40000, 50000, and 70000 cycles, it was decided that the crack was initiated between 50000 and 70000 cycles. For that reason, the signal under the 50000 cycle was chosen as the undamaged specimen signal. Then, the crack length was estimated using the proposed method. The results of the estimated crack lengths for specimen T8 are shown in Table 8.

Table 8. Estimated crack lengths for specimen T8

Cycles	40000	50000	70000	74883	76931
Estimated crack (mm)	0	0	1.37	1.94	2.51
Ground truth (mm)	0	0	0	1.94	2.5
Penalty Score $S(i)$	0	0	28.97	0	2.00

The prediction process for specimen T8 is the same as the prediction process for specimen T7, after considering the effect of variable loading through an additional preprocessing step. Figure 10 shows the constant and variable loading conditions. To consider the effect of variable loading, the equivalent effect of constant loading was calculated.

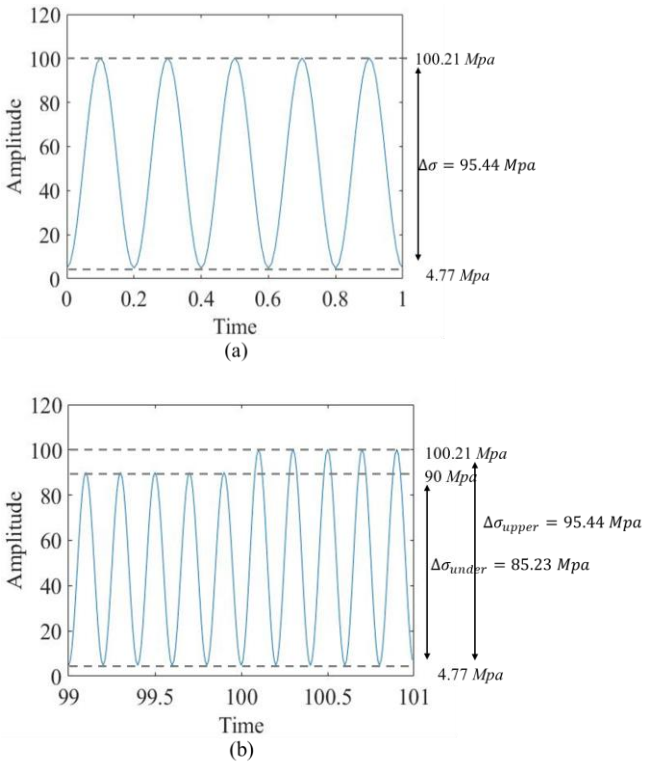

Figure 10. Summary of loading condition: (a) constant loading condition, (b) variable loading condition

To transform the variable loading condition into the equivalent effect of a constant loading condition, the average stress range of the lower- and upper-stress range was calculated. Then, the equivalent constant stress range was calculated using Eq. (18). Here, $\Delta\sigma_{\text{lower}}$ is the lower-stress range and $\Delta\sigma_{\text{upper}}$ is the upper-stress range. As a result, it was found that approximately 95% of the loading was applied, as compared to the constant loading condition, as shown in Eq. (19).

$$\Delta\sigma_{\text{variable}} = \frac{\Delta\sigma_{\text{lower}} + \Delta\sigma_{\text{upper}}}{2} \tag{18}$$

$$\Delta\sigma_{\text{variable}} \cong 0.95 \times \Delta\sigma_{\text{constant}} \tag{19}$$

Next, to examine the effect of the stress range on crack growth, Paris' law (Paris & Erdogan, 1963) was analyzed. Paris' law is defined as

$$\frac{da}{dN} = C(\Delta K)^m = C(Y\Delta\sigma\sqrt{\pi a})^m \tag{20}$$

$$\frac{da}{dN} \propto (\Delta\sigma)^m \tag{21}$$

where C and m are empirical parameters and ΔK is a stress intensity factor. From Paris' law, the effect of the stress range is reflected in the power of the empirical parameter, as shown in Eq. (21). Therefore, the effect of the variable loading on the training dataset can be applied by adjusting the cycle increment in the form of Eq. (22), under the same crack length increment.

$$dN' = (0.95)^{-m} dN \tag{22}$$

To calculate the empirical parameters of Paris' law, Markov Chain Monte Carlo (MCMC) simulation was used (Gilks, Richardson, & Spiegelhalter, 1995; Haario, Laine, Mira, & Saksman, 2006) with the training datasets. The results of the MCMC are summarized in Table 9.

Table 9. Summary of MCMC results

MCMC Algorithm	Delayed Rejection Adaptive Metropolis
Number of samples	100,000
m	2.0597
C	1.3826e-6

Using one of the empirical parameters, m, Eq. (22) was calculated as Eq. (23). However, this relationship is only valid in Region 2, as shown in Figure 11. Considering the nonlinear effect on Region 3 in the fatigue crack growth rate plot, the training dataset was modified using Eq. (24).

$$dN' = 1.11 \times dN \tag{23}$$

$$N^*(k) = N(k) \times (N(k)/N_0)^{1.11} \tag{24}$$

where N_0 is a cycle of crack initiation.

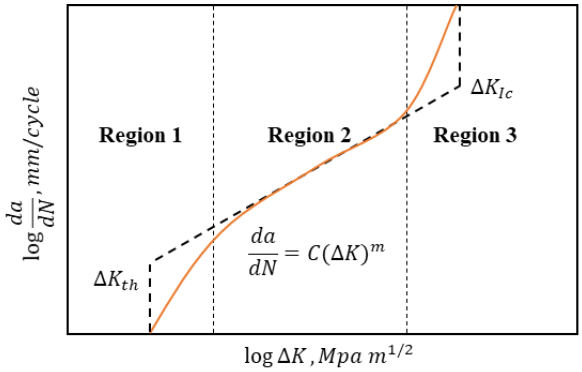

Figure 11. Fatigue crack growth rate

As a result, the cycles of specimens T3 and T4 were modified. The modified training datasets reflecting the effect of variable loading are shown in Figure 12.

The subsequent process is the same as the trans-fitting procedure used for specimen T7. First, the sum of two exponential functions (Exp2) was selected for specimen T4 and the sum of the Gaussian model and exponential function (Exp1+Gaussian1) was selected based on the statistical indicators of the goodness-of-fit. The results of the goodness-of-fit tests for the two candidate functions are given in Table

10. Second, along with the results of the goodness-of-fit test, training datasets were fitted to each of the selected candidate functions.

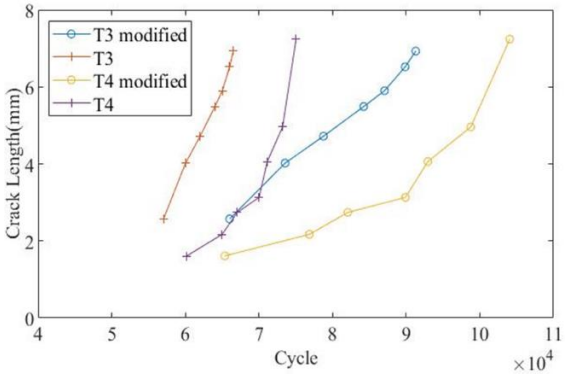

Figure 12. Modified training datasets

Table 10. Goodness-of-fit results for specimen T8

	T3		T4	
Candidates	SSE	DFE	SSE	DFE
Exp2 (E2)	0.3402	3	0.1796	3
Exp1+Gaussian1 (GE)	0.1276	2	0.2887	2

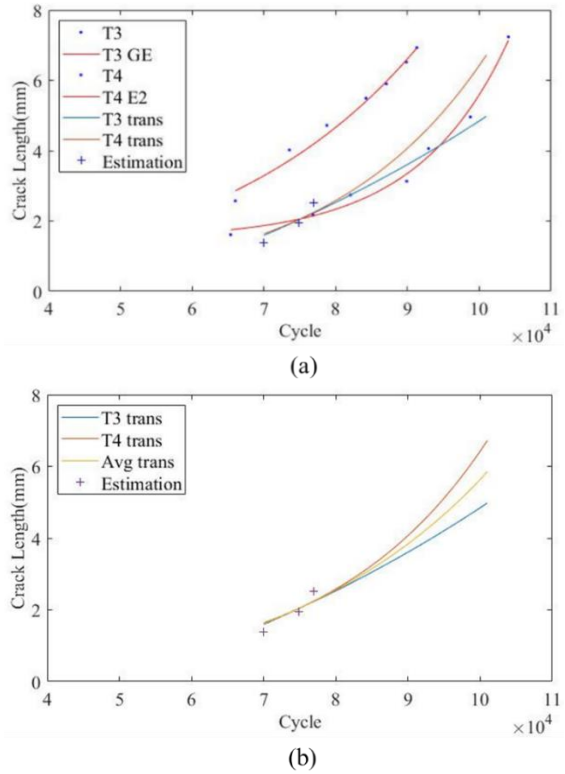

Figure 13. Results of curve translocating for specimen T8: (a) trans-fitting curve, (b) average trans-fitting curve

Third, the parameters of the fitting curve were updated. Figure 13 shows the results of the curve translocating process for specimen T8. The results of the fitting curves and trans-fitting curves are plotted in Figure 13(a). The average trans-fitting curve in Figure 13(b) were calculated through the average of the two trans-fitting curves. Finally, sequential updating was performed based on the crack length for the target cycle. Based on the first average trans-fitting curve, the results of sequential updating for the predicted crack length are shown in Figure 14.

From Figure 13(b) to Figure 14(d), there are five average trans-fitting curves. Each average trans-fitting curve can predict the crack lengths for the target cycles after the cycle used in the sequential updating process, as shown in Table 11. As was done in the case of specimen T7, the average value for all calculated values was adopted as the last prediction value.

Table 11. Predicted crack lengths for specimen T8

Cycle	89237	92315	96475	98492	100774
1st average trans-fitting curve	3.70	4.12	4.76	5.10	5.52
2nd average trans-fitting curve		4.06	4.65	4.96	5.34
3rd average trans-fitting curve			4.69	5.02	5.42
4th average trans-fitting curve				5.00	5.39
5th average trans-fitting curve					5.38
Final average value	3.70	4.09	4.70	5.02	5.41
Ground truth (mm)	3.71	3.88	4.61	4.96	5.52
Penalty Score $S(i)$	2.00	21.30	9.49	6.58	41.94

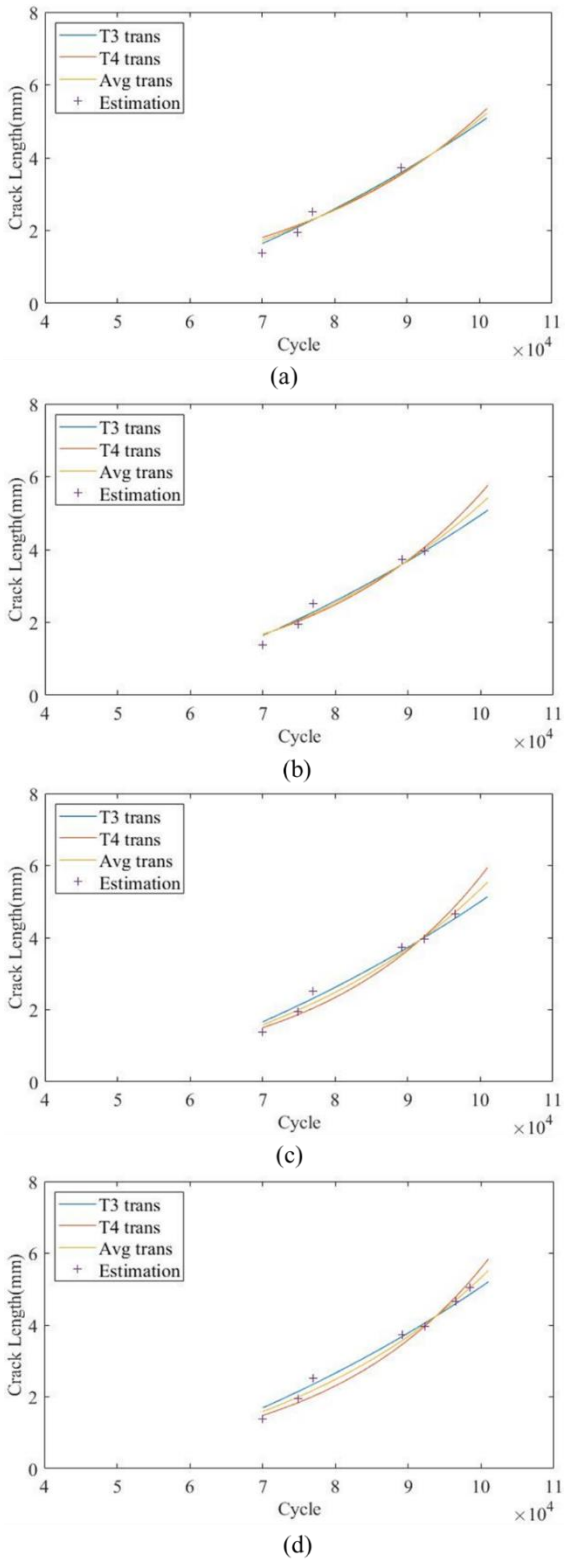

Figure 14. Sequential updated curves for specimen T8: (a) average trans-fitting curve for the second iteration, (b) average trans-fitting curve for the third iteration, (c) average trans-fitting curve for the fourth iteration, (d) average trans-fitting curve for the fifth iteration

5. CONCLUSION AND FUTURE WORK

In this study, a new method was proposed that consists of trans-fitting combined with SVR to estimate and predict a crack propagation trend using only the initial crack length of a target specimen. In the proposed method, the crack lengths were first estimated using an SVR model. To construct the regression model, the features were defined using filtered wave signals. Then, the crack lengths were predicted using the trans-fitting method, which adapted the crack propagation trend from the training datasets and applied it to the target datasets. The performance of the proposed method was demonstrated by using it on the given validation datasets. Through the validation process, crack propagation trends and wave signals of the training dataset were used to estimate the initial crack length of the target specimen and to accurately predict the crack propagation trend. Also, in the case of specimen exposed to variable loading, the proposed method was shown to be effective. The excellent performance of the proposed method resulted in it being ranked in first place in the 2019 PHM Conference Data Challenge.

Future extension of this research will include a sensitivity analysis to quantitatively analyze the impact of contamination on the training dataset. The proposed method in this paper was based on a data-driven approach; it has an inherent limitation of dependence on the training dataset. In future work, sensitivity analysis will be used to explore the effective contamination bounds of the training dataset. Additionally, as a case study in future research, validation of different materials and other types of failure modes will be performed to confirm the robustness of the proposed method.

ACKNOWLEDGMENT

This work was supported by the National Research Foundation of Korea (NRF) grant funded by the Korea Government (MSIT) (No. 2020R1A2C3003644)

REFERENCES

Adams, D., White, J., Rumsey, M., & Farrar, C. (2011). Structural health monitoring of wind turbines: method and application to a HAWT. *Wind Energy*, 14(4), 603-623. doi:10.1002/we.437

Agarwal, S., & Mitra, M. (2014). Lamb wave based automatic damage detection using matching pursuit and machine learning. *Smart materials and structures, 23*(8), 085012. doi10.1088/0964-1726/23/8/085012

Ahmad, W., Khan, S. A., Islam, M. M., & Kim, J.-M. (2019). A reliable technique for remaining useful life estimation of rolling element bearings using dynamic regression models. *Reliability Engineering and System Safety, 184*, 67-76. doi:10.1016/j.ress.2018.02.003

Benkedjouh, T., Medjaher, K., Zerhouni, N., & Rechak, S. (2013). Remaining useful life estimation based on nonlinear feature reduction and support vector regression. *Engineering Applications of Artificial*

Intelligence, *26*(7), 1751-1760. doi:10.1016/j.engappai.2013.02.006

Bishop, C. M. (2006). *Pattern recognition and machine learning. springer*.

Bozchalooi, I. S., & Liang, M. (2008). A joint resonance frequency estimation and in-band noise reduction method for enhancing the detectability of bearing fault signals. *Mechanical Systems and Signal Processing*, *22*(4), 915-933. doi:10.1016/j.ymssp.2007.10.006

Brownjohn, J. M. (2006). Structural health monitoring of civil infrastructure. *Philosophical Transactions of the Royal Society A: Mathematical, Physical Engineering Sciences*, *365*(1851), 589-622. doi:10.1098/rsta.2006.1925

Coelho, C. K., Das, S., Chattopadhyay, A., Papandreou-Suppappola, A., & Peralta, P. (2007). Detection of fatigue cracks and torque loss in bolted joints. *In Health Monitoring of Structural and Biological Systems* 2007, 6532, 653204. doi:10.1117/12.715984

Conn, A. R., Gould, N. I., & Toint, P. L. (2000). *Trust region methods* (Vol. 1): Siam.

Forman, R. G., Kearney, V., & Engle, R. (1967). Numerical analysis of crack propagation in cyclic-loaded structures. *Journal of basic engineering*, *89*(3), 459-463. doi:10.1115/1.3609637

Gilks, W. R., Richardson, S., & Spiegelhalter, D. (1995). *Markov chain Monte Carlo in practice*: Chapman and Hall/CRC.

Haario, H., Laine, M., Mira, A., & Saksman, E. (2006). DRAM: efficient adaptive MCMC. *Statistics and computing*, *16*(4), 339-354. doi:10.1007/s11222-006-9438-0

Janapati, V., Kopsaftopoulos, F., Li, F., Lee, S. J., & Chang, F. K. (2016). Damage detection sensitivity characterization of acousto-ultrasound-based structural health monitoring techniques. *Structural Health Monitoring*, 15(2), 143-161. doi: 10.1177/1475921715627490

Kessler, S. S., Spearing, S. M., & Soutis, C. (2002). Damage detection in composite materials using Lamb wave methods. *Smart materials and structures*, *11*(2), 269. doi:10.1088/0964-1726/11/2/310

Lee, J., Wu, F., Zhao, W., Ghaffari, M., Liao, L., & Siegel, D. (2014). Prognostics and health management design for rotary machinery systems—Reviews, methodology and applications. *Mechanical systems and signal processing*, *42*(1-2), 314-334. doi:10.1016/j.ymssp.2013.06.004

Liu, M., Frangopol, D. M., & Kwon, K. (2010). Fatigue reliability assessment of retrofitted steel bridges integrating monitored data. *Structural Safety*, *32*(1), 77-89. doi:10.1016/j.strusafe.2009.08.003

Neerukatti, R. K., Hensberry, K., Kovvali, N., & Chattopadhyay, A. (2016). A novel probabilistic approach for damage localization and prognosis including temperature compensation. *Journal of Intelligent Material Systems and Structures*, *27*(5), 592-607. doi:10.1177/1045389X15575084

Oppenheim, A. V. (1999). *Discrete-time signal processing*: Pearson Education India.

Ostachowicz, W., & Güemes, A. (2013). *New trends in structural health monitoring* (Vol. 542): Springer Science & Business Media.

Paris, P., & Erdogan, F. (1963). A critical analysis of crack propagation laws. *Journal of basic engineering*, *85*(4), 528-533. doi:10.1115/1.3656900

Peng, T., Liu, Y., Saxena, A., & Goebel, K. (2015). In-situ fatigue life prognosis for composite laminates based on stiffness degradation. Composite Structures, 132, 155-165. doi:10.1016/j.compstruct.2015.05.006

Qiu, L., Liu, M., Qing, X., & Yuan, S. (2013). A quantitative multidamage monitoring method for large-scale complex composite. *Structural Health Monitoring*, 12(3), 183-196. doi:10.1177/1475921713479643

Salcedo-Sanz, S., Ortiz-Garcı, E. G., Pérez-Bellido, Á. M., Portilla-Figueras, A., & Prieto, L. (2011). Short term wind speed prediction based on evolutionary support vector regression algorithms. *Expert Systems with Applications*, *38*(4), 4052-4057. doi:10.1016/j.eswa.2010.09.067

Staszewski, W., Mahzan, S., & Traynor, R. (2009). Health monitoring of aerospace composite structures–Active and passive approach. *composites Science and Technology*, *69*(11-12), 1678-1685. doi:10.1016/j.compscitech.2008.09.034

Tinga, T., & Loendersloot, R. (2014). Aligning PHM, SHM and CBM by understanding the physical system failure behaviour, *Proceedings of the European Conference of the Prognostics and Health Management Society*, 162-171.

Tipping, M. E. (2003). Bayesian inference: An introduction to principles and practice in machine learning. In *Summer School on Machine Learning*, 41-62. doi:10.1007/978-3-540-28650-9_3

Walker, H. M. (1940). Degrees of freedom. *Journal of Educational Psychology*, *31*(4), 253. doi:10.1037/h0054588

Walker, K. (1970). The effect of stress ratio during crack propagation and fatigue for 2024-T3 and 7075-T6 aluminum. In *Effects of environment and complex load history on fatigue life*: ASTM International. doi: 10.1520/STP32032S

Yang, Y., Ng, C.-T., & Kotousov, A. (2018). Influence of crack opening and incident wave angle on second harmonic generation of Lamb waves. *Smart Materials and Structures*, *27*(5), 055013. doi: 10.1088/1361-665X/aab867

BIOGRAPHIES

Myeongbaek Youn received the B.S. from Sungkyunkwan University, Seoul, Republic of Korea, in 2018. He is currently pursuing the Ph.D. degree in the Department of Mechanical and Aerospace Engineering in Seoul National University, Seoul, Republic of Korea. His current research topics include prognostics and health management for electric machines using a signal processing approach.

Yunhan Kim received his B.S. degree from Seoul National University, Seoul, Republic of Korea, in 2016. He is a Ph.D. student in the Department of Mechanical and Aerospace Engineering in Seoul National University. His research topic is prognostics and health management for rotating systems.

Dongki Lee received the B.S. degree from Hanyang University, Seoul, Republic of Korea, in 2013 and the M.S. degree from Seoul National University, Seoul, Republic of Korea, in 2018. He is currently working for LG Electronics. His current research topics include prognostics and health management for motors.

Minki Cho received the M.S. degree in Acoustical Engineering from University of Southampton, The United Kingdom, in 2017. He is currently working for LG Electronics. His research interests relate to vibration analysis and applications of acoustics and prognostics and health management for rotating system.

Byeng Dong Youn received the B.S. degree in mechanical engineering from Inha University, Incheon, South Korea, in 1996, the M.S. degree in mechanical engineering from Korea Advanced Institute of Science & Technology, Daejeon, South Korea, in 1998, and the Ph.D. degree in mechanical engineering from the University of Iowa, Iowa City, IA, USA, in 2001. He is a Professor in the Department of Mechanical and Aerospace Engineering, Seoul National University, Seoul, South Korea. Dr. Youn was the recipient of ASME IDETC Best Paper Awards (2001 and 2008), the ISSMO/Springer Prize for a Young Scientist (2005), the IEEE PHM Competition Winner (2014), the PHM Society Data Challenge Competition Winner (2014, 2015, 2017), etc.